Dependence of the populations of low-energy levels in ^{108,110}Ag on the resonance spin and parity

L. Zanini* and F. Corvi
CEC-JRC, Institute for Reference Materials and Measurements, B-2440 Geel, Belgium

H. Postma
Delft University of Technology, P.O. Box 5046, NL-2600 GA Delft, The Netherlands

F. Bečvář
Faculty of Mathematics and Physics, Charles University in Prague, V Holešovičkách 2, CZ-18000 Prague 8, Czech Republic
(Received 11 January 2000; published 21 April 2000)

Measurements of prompt γ rays, following neutron capture in ^{107}Ag and ^{109}Ag have been performed at the GELINA facility in the resonance energy region up to about 1 keV. From the intensities of low- and high-energy γ rays the spins of 53 ^{107}Ag and 78 ^{109}Ag *s*- and *p*-wave resonances have been assigned. These spectroscopic quantities are important for the interpretation of data from parity violation experiments performed by the TRIPLE Collaboration. The intensities of low-energy transitions showed a dependence not only on the spin of the resonance but also on its parity. This effect allows the assignment of the parity of the resonances and may open new perspectives in the study of the γ decay of the compound nucleus.

PACS number(s): 21.10.Hw, 24.60.Dr, 27.60.+j, 29.30.Kv

I. INTRODUCTION

The strong enhancement of parity violation (PV) effects in the compound nucleus system has been extensively studied by the TRIPLE Collaboration at the Los Alamos National Laboratory during the past ten years [1,2]. After having examined PV effects in heavy nuclei such as ^{238}U and ^{232}Th [3,4], more attention was concentrated on isotopes in the $3p$ peak region of the *p*-wave neutron strength function, such as ^{106}Pd, ^{108}Pd, ^{107}Ag, ^{109}Ag, ^{113}Cd, and ^{115}In [5,6].

For a more precise determination of the quantities related to PV effects, it is necessary to know the spins and parities of the neutron resonances, especially in the case of nonzero target nuclei. As a part of the efforts to meet these demands, the aim of the present work was to determine spins and parities for a large number of resonances of ^{107}Ag and ^{109}Ag up to about 1 keV, i.e., in the energy range of interest for PV studies, using capture gamma-ray spectroscopic methods based on the study of low- and high-energy γ rays.

In medium and heavy nuclei, where the level density is high, it can be assumed that the statistical model applies for the γ decay of the compound nucleus, although nonstatistical effects must sometimes be considered [7,8]. Therefore the decay properties are determined mainly by the level density and the photon strength functions. The γ decay from the capture state to the ground level usually happens in no more than 3–4 steps. The high-energy part of the primary spectrum may be observed, and in principle, and often in practice, it is possible to determine the spin and parity of a resonance from the observation of primary γ rays which directly feed levels with known spin and parity. However, for very small *p*-wave resonances it can be very difficult or impossible to make a definitive assignment, because of the limited statistics available for high-energy γ rays. Therefore one might consider the γ transitions which arise from the low-energy levels, typically below 1 MeV. These levels are populated via the cascade process, but since the average multiplicity is low, information on spectroscopic quantities of the initial state (the resonance) may still be present, and easily observable thanks to the high intensity of the low-energy transitions, and to the high efficiency of germanium detectors in this energy range.

Besides the link with studies of parity violation, it is of interest to investigate low- and high-energy γ rays in *p*-wave neutron capture as they relate to the statistical γ decay of the compound nucleus. Gamma rays from *p*-wave neutron capture have not been studied extensively in the past, and one can better investigate these decay properties by considering the γ rays from resonances with different initial spin and parity. Both ^{107}Ag and ^{109}Ag target nuclei have $I^{\pi}=\frac{1}{2}^{-}$; thus *s* resonances can assume $J^{\pi}=0^{-},1^{-}$, while *p* resonances can have $J^{\pi}=0^{+},1^{+},2^{+}$.

The low average multiplicity in the γ-cascade decay and the predominantly dipole character of the emitted radiation constitute the physical basis of the *low-level population method* of resonance spin assignment, according to which low-energy levels with higher (lower) spins are more populated in resonances with higher (lower) spins. This method has been successfully applied to the study of *s* resonances [9,10], and recently extended to the analysis of *p*-wave resonances [11].

Concerning the parity assignment, the dependence of the populations of low-energy levels is very difficult to predict, since $E1$ and $M1$ transitions play competitive roles and the knowledge of the behavior of the corresponding photon strength functions is still far from being adequately understood. Studying the parity dependence of the low-energy populations is therefore of great interest not only for the

*Present address: Los Alamos National Laboratory, Los Alamos, NM 87545.

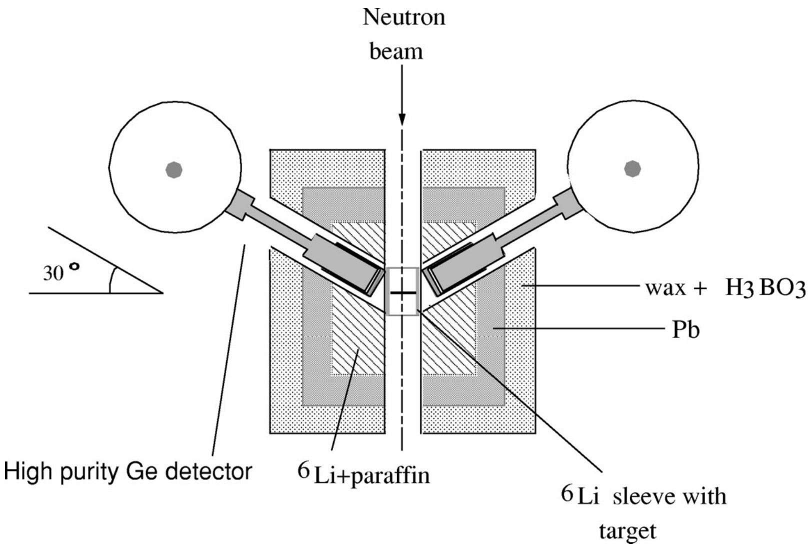

FIG. 1. Schematic view of the experimental setup.

reason that these populations might provide a basis for the parity assignment of neutron resonances, but also for getting additional information on the level densities and photon strength functions.

II. RESONANCE SPIN AND PARITY ASSIGNMENT

A. Experimental procedure

Resonance neutron capture measurements were performed at the GELINA pulsed neutron source facility [12,13] at the Institute for Reference Materials and Measurements in Geel, Belgium. The linear accelerator was operated to produce 1 ns wide pulses of electrons with 100 MeV average energy at a repetition frequency of 800 Hz. The average electron current was about 75 μA. Neutrons were produced by the interaction of the electrons with a rotating uranium target. A moderator consisting of water inside a beryllium box was placed close to the uranium target to increase the number of slow neutrons. The sample was placed at a distance of 12.8 m from the neutron source, having in this way a relatively high neutron flux [about $9\times10^3/E^{0.9}$ n/(cm^2 s eV)] and sufficient neutron energy resolution in the energy range of interest. Measurements were performed on two enriched samples, both on loan from the ORNL Isotope Pool: one consisted of 49.8 g of an enriched (98.3%) ^{107}Ag metal powder packed in an aluminum box, forming a disc of 8.9 cm diameter with walls 0.05 cm thick. The other one was a disc of 10 cm diameter and 50 g mass of Ag enriched in ^{109}Ag to 97.1%. Each sample was placed perpendicular to the beam (see Fig. 1). Incident neutron energies were determined by time of flight over the flight path length. Capture γ rays were viewed by two coaxial intrinsic germanium detectors of 70% efficiency (relative to the ^{60}Co lines), placed backward at a distance of about 15 cm from the sample center and at an angle of 120° with respect to the neutron direction. In order to prevent detection of scattered neutrons, discs about 4 cm thick made of wax and ^{6}Li carbonate were inserted between sample and detectors. The entire structure was contained inside a shielding made of lead and borated wax bricks each 10 cm thick. Capture γ rays in the energy range from 0.1 MeV up to about 7 MeV were measured with two 8k ADCs in the neutron energy range from 10 eV to about 1 keV, for a measuring time of about 1000 h. Data were recorded in list mode, writing for each event TOF and ADC values, using the data acquisition program FAST [14].

The TOF spectrum for ^{109}Ag(n,γ) is shown in Fig. 2. From the recorded event data, capture γ-ray spectra corresponding to selected TOF intervals were sorted out, each one being associated with a single neutron resonance or with a background region between two resonances. In order to obtain the pure capture yield of a given resonance, the γ spectrum corresponding to one or more nearby background regions was subtracted from the raw data after proper normalization. In case of unresolved resonances, the capture yield was fitted with the shape program FANAC [15]: for each resonance the fraction f of a nearby resonance in the given TOF interval was determined and the corresponding γ-ray spectrum was subtracted. This procedure was applied to the ^{107}Ag resonances at 64.24, 64.74, 125.1, and 126.1 eV, and to the ^{109}Ag resonances at 32.7, 164.3, 169.8, 199.0, 219.2, 264.7, 293.3, 360.4, 391.6, 441.0, 446.5, 557.2, 560.7, 1057, and 1062 eV. In addition to the increase of the statistical uncertainty due to background subtraction, such a procedure introduces additional uncertainties in the resulting pure spectrum. The uncertainty in the calculated f was evaluated considering those resonances which were superimposed on strong resonances of the other isotope; in fact, in this case the exact fraction can be determined since the γ lines of the contaminating resonance must disappear. By comparing the fraction evaluated with this procedure with the one calculated we estimated an uncertainty in f of about 10%.

Examples of typical low-energy γ spectra are shown in Fig. 3 for five ^{109}Ag resonances. The spectra were analyzed with the fit program PROFIT [16]. The peaks in the low-energy region were fitted using Gaussian functions, each Gaussian being convoluted with a smoothed step function in order to account for a slightly higher background on the low energy side of the peak, due to Compton scattering of photons into the detector and the escape of photoelectrons from

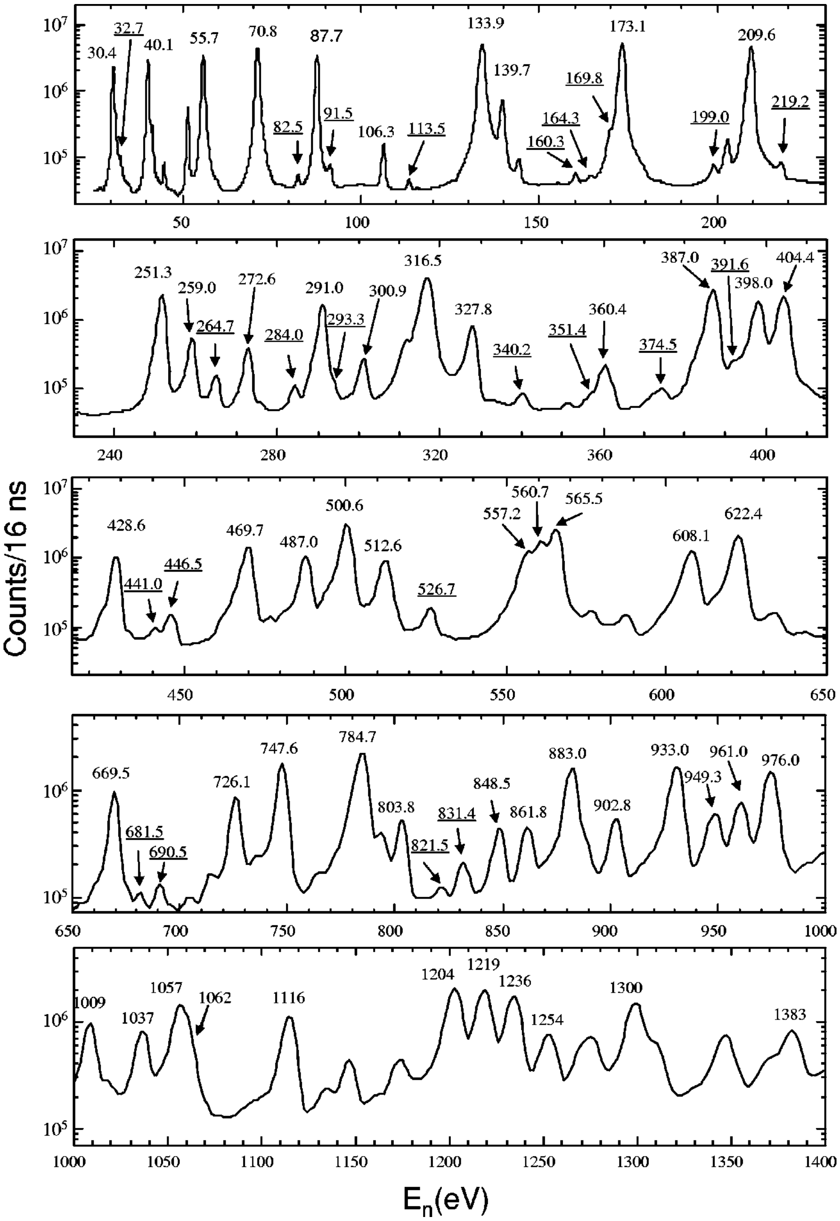

FIG. 2. Time-of-flight spectrum for $^{109}\mathrm{Ag}(n,\gamma)^{110}\mathrm{Ag}$ up to 1.4 keV. Resonance energies are indicated; underlined numbers indicate *p*-wave resonances.

the Ge crystals; the fitting formula from Ref. [17] was adopted:

$$y = \mathrm{A}\left[\frac{1}{\sqrt{2\pi}\sigma}\exp\left(-\frac{(E-E_c)^2}{2\sigma^2}\right) + \mathrm{B}\,\mathrm{erfc}\left(\frac{E-E_c}{\sqrt{2}\sigma}\right)\right], \tag{1}$$

where $\mathrm{erfc}(x)$ is the complementary error function and accounts for the step function.

B. Parity assignments

The assignment of the parity of a resonance is often performed on the basis of its neutron width. A statistical approach, based on the Bayes' theorem on conditional probabilities [20], was developed by Bollinger and Thomas [21] and has been used for parity assignments (see for instance Refs. [22–24]). Clearly, a statistical approach is not expected to be completely reliable.

With an attempt to assign the resonance parities with a higher level of confidence, we have studied the dependence of the intensities of low-energy transitions on the parity of the resonance. Wherever available, we have also used information from high-energy transitions. In this section we first describe the resonance parity assignment based on spectroscopic methods. The results are then compared with what we obtained applying the Bayes' theorem on the observed values of $g\Gamma_n$.

1. Spectroscopic methods

As previously mentioned, the dependence of the populations of low-energy levels on the resonance parity has not been studied in the past; in fact, few measurements of γ rays from *p*-wave capture have been performed. Moreover, in order to investigate such a dependence, it is necessary that the compound nucleus has strongly populated low-energy levels of both parities, which is not always the case. In the case of

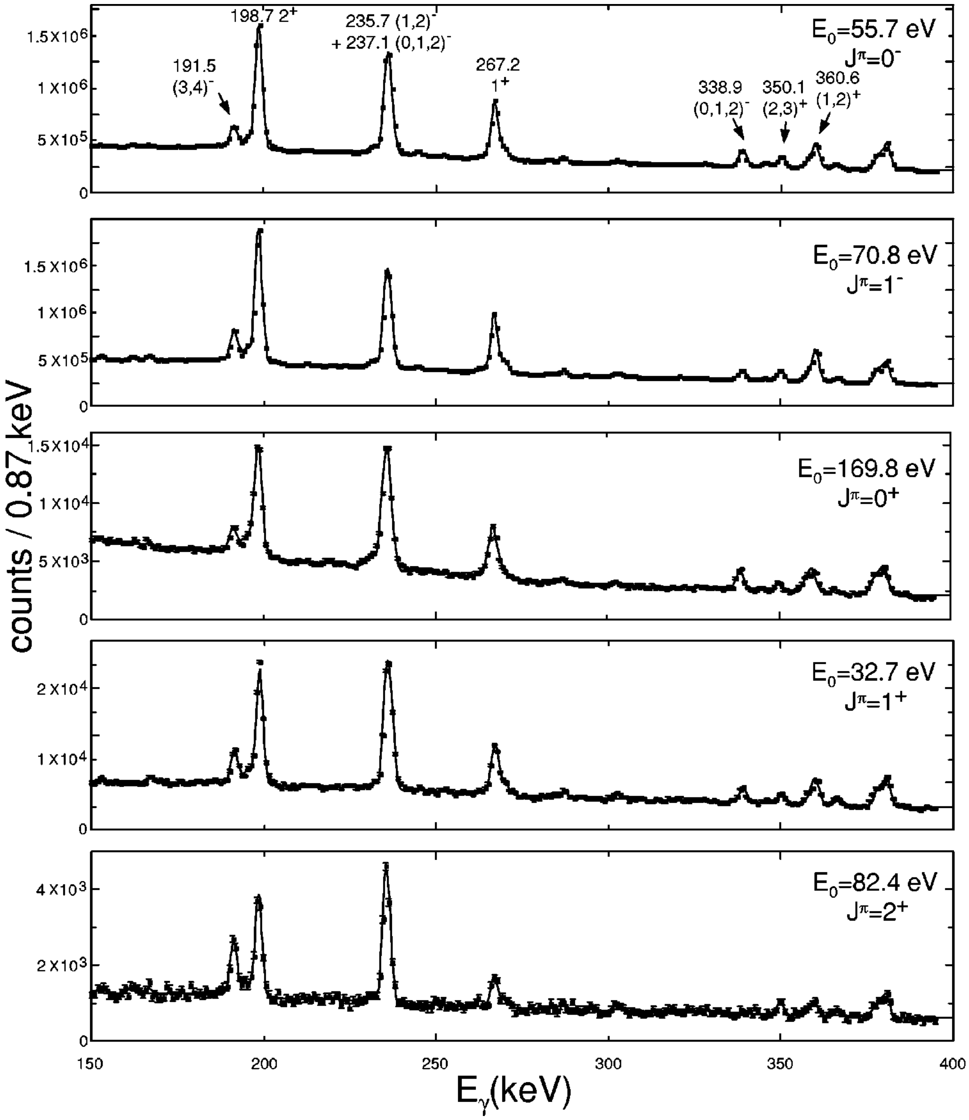

FIG. 3. Low-energy γ spectra for five ^{109}Ag resonances of different spin and parity. The energies of the stronger transitions are given in keV. For each transition the spin and parity of the initial level, after Refs. [18,19], is given. The energies, spins, and parities of the resonances are also indicated.

the ^{108}Ag and ^{110}Ag compound nuclei, strong low-energy transitions from levels of opposite parity are present, making these transitions ideal for such investigations.

As a first step, we analyzed low-energy parts of the γ-ray spectra belonging to well-isolated resonances of both parities to which a value $J=1$ had been unambiguously assigned, using the methods described in the next section. From this analysis we deduced average intensities of the most intense low-energy transitions. It turned out from these data that those low-lying levels, the parity of which is opposite to the parity of the neutron capturing state, display a marked tendency to be populated more strongly than the levels with the other parity. This can be seen from Figs. 4 and 5, where for each transition the ratio between the average intensities for *s* and *p* resonances is plotted. The observed effect is about 40%. If this effect, established for a limited set of transitions, is due to average statistical properties of the cascade decay of the compound nucleus, it will certainly persist in the cases of all remaining transitions between the low-lying levels.

The properties of the cascade decay of the compound nucleus are described by the nuclear level density and the photon strength functions. In particular, the $E1$ and $M1$ photon strength functions are playing a dominant role [25]. Since $E1$ and $M1$ transitions have different parities, they may be responsible for the observed parity effect. Also an effect from a possible parity dependence of the level density should not be neglected. With an attempt to understand the observed effect in terms of photon strength functions, a special experiment devoted to studying two-step cascades, following the thermal neutron capture in ^{107}Ag, has been undertaken at the dedicated facility in Řež [26]. The obtained results will be published separately [27].

The parity effect could be exploited for an assignment of the parity of the resonances. Since the results for ^{107}Ag have been already partially shown in Ref. [5], in this and in the following section we concentrate mainly on ^{109}Ag. In Fig. 6

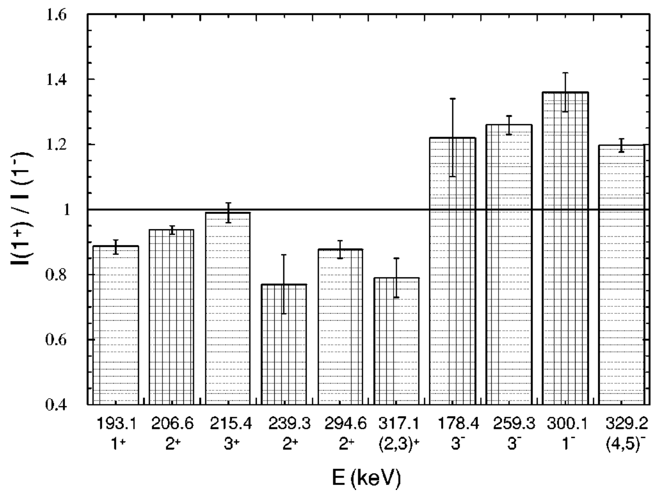

FIG. 4. The parity effect in ^{107}Ag resonances. Each bar represents the ratio between the intensities of the indicated γ transition from p resonances with $J^{\pi}=1^{+}$ and s resonances with $J^{\pi}=1^{-}$. These intensities are the averages from several resonances.

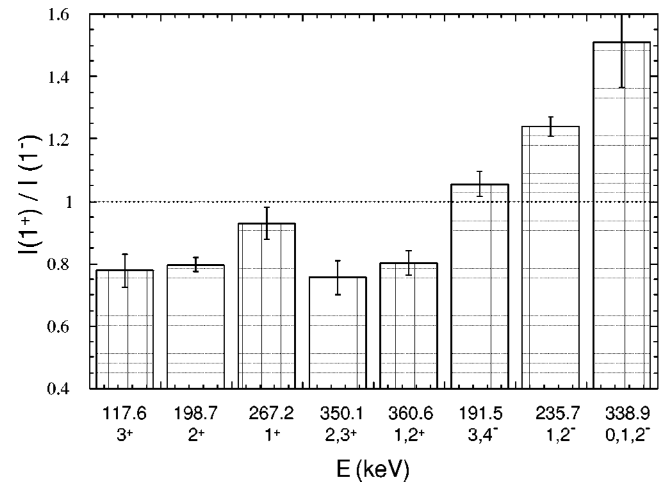

FIG. 5. Same as Fig. 4 but for ^{109}Ag resonances.

the ratio between the intensity of the transition of 198.7 keV (deexciting a level with $J^{\pi}=2^{+}$) and the intensity of the doublet at 235.7 and 237.1 keV (deexciting two levels with negative parity) is plotted for all the ^{109}Ag resonances with $J=0$ and $J=1$. For each set of data a clear separation in two

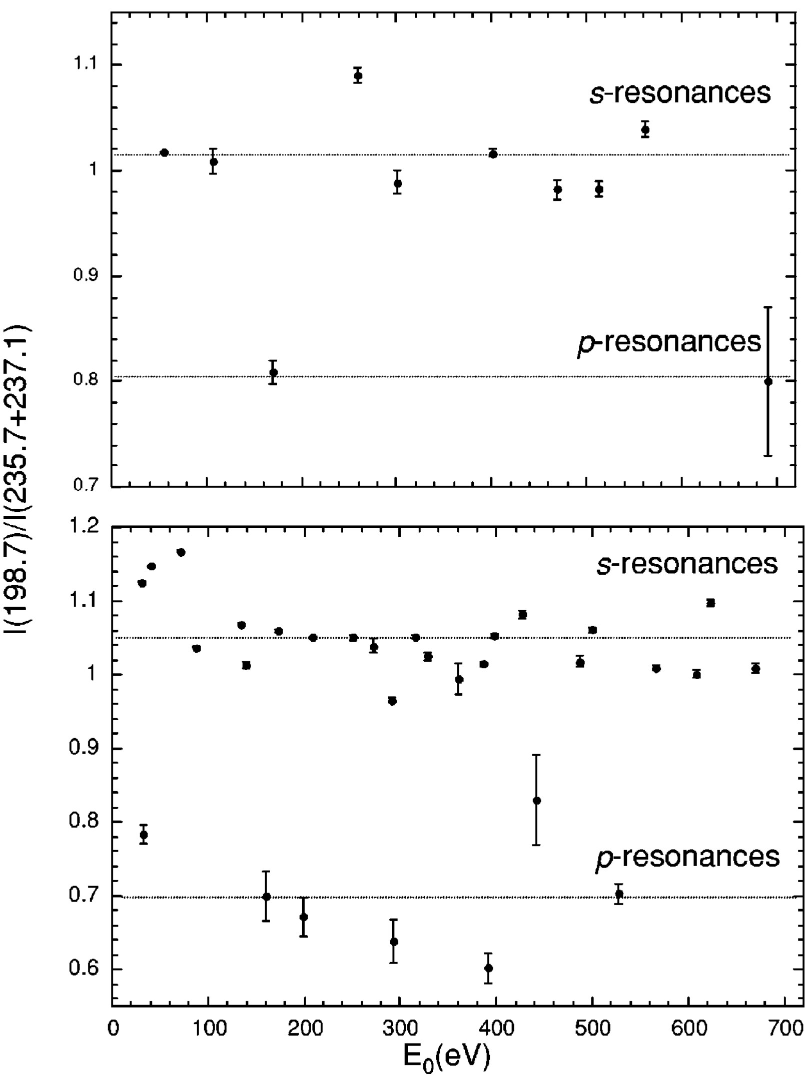

FIG. 6. Ratios of the intensities between the indicated γ lines for $J=0$ (top) and $J=1$ (bottom) ^{109}Ag resonances, as a function of the resonance energies. The dashed lines are the average values for the various groups of resonances.

groups is observed. To the upper group $\ell=0$ is assigned, while to the lower group we assign $\ell=1$. This assignment is justified from the fact that all the resonances with higher value of $g\Gamma_n$ are in the upper groups.

Additional support to this assignment can be obtained in the intensities of the high-energy transitions from the capture state to low-energy levels of known parity. In this case it is assumed that above 6 MeV the $E1$ transitions are significantly stronger than the $M1$. As shown in Ref. [28], in this energy range the ratio between $E1$ and $M1$ photon strength functions is about 7 for ^{107}Ag. If a similar ratio holds also for ^{109}Ag, observation in a resonance of strong primary transitions to low-energy levels with a given parity leads to assignment of opposite parity to the resonance. However, this method must be used with caution: in the case of weak resonances the number of observed primary transitions is small and their deduced intensities are subject to large statistical uncertainties. In these cases the parity using primary transitions was determined only tentatively, or not at all. Wherever available, the information from high-energy γ rays led to parity assignments completely consistent with those obtained from low-energy γ rays, for both ^{107}Ag and ^{109}Ag.

The orbital angular momentum values, assigned following these procedures, are summarized in Tables I and II.

2. Analysis based on Bayes' theorem

It is interesting to compare the results in Tables I and II with those following from the statistical analysis of parameters $g\Gamma_{\mathrm{n}}$ based on the application of Bayes' theorem. It is tacitly assumed that all experimentally accessible values of $g\Gamma_{\mathrm{n}}$ with generally *unknown* statistical factors g belong exclusively to neutron resonances with neutron orbital momenta $\ell=0,1$.

The *a posteriori* probability $P(\ell|g\Gamma_{\mathrm{n}})$ that a given resonance with the measured value of $g\Gamma_{\mathrm{n}}$ is excited by neutrons with orbital momentum ℓ is

$$P(\ell|g\Gamma_{\mathrm{n}})=\frac{P(g\Gamma_{\mathrm{n}}|\ell)P(\ell)}{P(g\Gamma_{\mathrm{n}}|1)P(1)+P(g\Gamma_{\mathrm{n}}|0)P(0)}, \tag{2}$$

where $P(\ell)$ is the *a priori* (unconditional) probability that a randomly selected neutron resonance belongs to neutrons with orbital momentum ℓ, while $P(g\Gamma_{\mathrm{n}}|\ell)$ is the probability density for the random variable $x\equiv g\Gamma_{\mathrm{n}}$, given the neutron orbital momentum ℓ.

For $\ell=1$ Eq. (2) can be formally rewritten to

$$P(1|g\Gamma_{\mathrm{n}})=\left[1+\kappa\frac{P(g\Gamma_{\mathrm{n}}|0)}{P(g\Gamma_{\mathrm{n}}|1)}\right]^{-1}, \tag{3}$$

where

$$\kappa=\frac{P(0)}{P(1)}. \tag{4}$$

If we assume that the density of nuclear levels near the neutron threshold for each value of their spin J is parity independent, then

$$\kappa=\sum_{J=|I-1/2|}^{I+1/2} f(J)\left[\sum_{J'=||I-1/2|-1|}^{I+3/2} f(J')\right]^{-1}, \tag{5}$$

where $f(J)$ is the spin-dependent factor of the level-density formula and I is the target spin.

In the general case the probability density $P(g\Gamma_{\mathrm{n}}|0)$ is formed by a linear combination of two separately rescaled probability densities describing the χ^2 distribution with the number of degrees of freedom $\nu=1$. Under the assumption of absence of spin-orbit splitting of the neutron strength function S_ℓ for $\ell=1$, the so-called *neutron pole* strength function does not depend on the channel spin, see Refs. [29,30]. In this case the probability density $P(g\Gamma_{\mathrm{n}}|1)$ is formed generally by a linear combination of four separately rescaled probability densities for χ^2: two of them belong to the number of degrees of freedom $\nu=1$ and the other two to $\nu=2$.

For targets of ^{107}Ag and ^{109}Ag, for which $I=1/2$, the probability density $P(g\Gamma_{\mathrm{n}}|1)$ involves two χ^2 distributions with $\nu=1$ and only one with $\nu=2$, while $P(g\Gamma_{\mathrm{n}}|0)$ is formed by both χ^2 distributions with $\nu=1$. For these nuclei

$$P(g\Gamma_{\mathrm{n}}|0)=\sum_{J=0,1}\alpha_J\,\omega_{0J}\left(\frac{1}{2\pi\xi_{0J}}\right)^{1/2}\exp\left(-\frac{1}{2}\xi_{0J}\right) \tag{6}$$

and

$$P(g\Gamma_{\mathrm{n}}|1)=\frac{1}{2}\beta_1\,\omega_{11}\exp\left(-\frac{1}{2}\xi_{11}\right)+\sum_{J=0,2}\beta_J\,\omega_{1J}\left(\frac{1}{2\pi\xi_{1J}}\right)^{1/2}\exp\left(-\frac{1}{2}\xi_{1J}\right), \tag{7}$$

where

$$\alpha_J=f(J)\left[\sum_{J'=0}^{1} f(J')\right]^{-1},\quad \beta_J=f(J)\left[\sum_{J'=0}^{2} f(J')\right]^{-1}, \tag{8}$$

and

$$\omega_{\ell J}=\left(\frac{1\ \mathrm{eV}}{E_{\mathrm{n}}}\right)^{1/2}\frac{kR}{g_J P_\ell D_J S_\ell}. \tag{9}$$

Here, E_{n} is the energy of the resonance, k is the corresponding wave number, R is the channel radius, g_J is the *known* statistical factor for resonances with spin J (as opposed to the factor g), P_ℓ is the neutron penetrability factor, see, e.g., [31], and D_J is the average spacing between neighboring resonances with a fixed J^π.

The random variable of interest, $x\equiv g\Gamma_n$, enters the right-hand sides of Eqs. (6) and (7) via dimensionless variables $\xi_{\ell J}$. Specifically,

$$\xi_{\ell J}=\omega_{\ell J}\,x. \tag{10}$$

TABLE I. Spin and parity assignment of ^{107}Ag resonances following different methods. The Bayesian probabilities (BP) are given. Under the columns with suffixes HE and LE the ℓ and J assignments from high-energy and low-energy γ-ray methods are indicated, respectively. Under the column J^a are the spin values from Ref. [34]. The adopted values are those with the suffix LE. Resonance energies and neutron widths are taken from Refs. [5,33].

E_0 (eV)	$g\Gamma_n$ (meV)	BP	ℓ_{HE}	ℓ_{LE}	J^a	J_{HE}	J_{LE}	E_0 (eV)	$g\Gamma_n$ (meV)	BP	ℓ_{HE}	ℓ_{LE}	J^a	J_{HE}	J_{LE}
16.3	2.9 ± 0.2	0.0000	0	0	0		0	310.8	65 ± 15	0.0000	0	0	1	1	1
41.57	2.8 ± 0.4	0.0000	0	0	1	1	1	328.2	0.60 ± 0.10	0.7609	1	1		2	2
44.90	0.62 ± 0.1	0.0000	0	0	0	1	1	346.8	0.40 ± 0.04	0.8875	0	0		1	1
51.56	17.9 ± 1.8	0.0000	0	0	1	1	1	361.2	15.5 ± 1.0	0.0000	0	0	1	1	1
64.24	0.018 ± 0.002	0.9706	1	1		1,2	1	381.8	0.29 ± 0.03	0.9262	0	0		1	1
64.74	0.013 ± 0.001	0.9756	1	1		1,2	2	403.9	0.30 ± 0.08	0.9270		1			1
73.21	0.027 ± 0.006	0.9631	1	1		1,2	1	409.2	0.36 ± 0.05	0.9166		1			2
83.55	0.015 ± 0.002	0.9748		1			2	422.5	0.18 ± 0.02	0.9443	1	1		(1,2)	0
107.6	0.014 ± 0.002	0.9742	1	1		1,2	1	444.0	21.3 ± 2.0	0.0000	0	0			0
110.8	0.081 ± 0.009	0.9209	1	1		1,2	2	460.9	18.0 ± 2.0	0.0000		0		1	1
125.1	0.010 ± 0.001	0.9736	1	1			0	466.8	63.0 ± 5.0	0.0000	0	0	1	1	1
126.1	0.018 ± 0.002	0.9721		1			1	472.4	14.0 ± 1.2	0.0000	0	0			0
128.5	0.092 ± 0.009	0.9261	1	1		1,2	2	494.9	0.40 ± 0.08	0.9209		1			2
144.2	4.0 ± 0.8	0.0000	0	0	0		0	514.7	50.0 ± 5.5	0.0000	0	0		1	1
154.8	0.025 ± 0.003	0.9691		1			1	531.2	0.4 ± 0.2	0.9237	1	1			1
162.0	0.28 ± 0.02	0.6525	0	0		1	1	553.8	163 ± 30	0.0000	0	0	0		0
166.9	0.19 ± 0.01	0.8586	0	0			0	575.8	9.0 ± 4.0	0.0000	0	0	1	1	1
173.7	5.5 ± 0.5	0.0000	0	0			1	586.9	96.2 ± 0.1	0.0000	0	0	0	1	1
183.5	0.13 ± 0.01	0.9309	1	1		1	1	607.3	2.82 ± 0.6	0.2055	1	1		2	2
202.6	12.9 ± 0.5	0.0000	0	0	1		1	624.9	16 ± 3	0.0000	0	0		1	1
218.9	0.084 ± 0.008	0.9554	1	1		(1,2)	1	652.5	12.4 ± 2	0.0000	0	0			1
228.3	0.040 ± 0.004	0.9633		1			2	673.7	63.7 ± 0.1	0.0000	0	0		1	1
231.0	0.052 ± 0.004	0.9617		1			2	694.8	14.9 ± 1.6	0.0000	0	0		1	1
251.3	16 ± 4	0.0000	0	0		1	1	702.1	2.9 ± 0.3	0.3577	1	1		1,2	2
259.9	0.25 ± 0.03	0.9055	1	1		1,2	1	751.8	66.2 ± 0.1	0.0000	0	0		1	1
264.5	2.5 ± 0.2	0.0000	0	0		1	1	778.8	9.14 ± 0.1	0.0005	0	0			1
269.9	0.20 ± 0.02	0.9288	1	1		1	1								

Under the conditions of a real experiment only intense enough resonances are observable. As a result, only those values of $g\Gamma_{\rm n}$ that exceed a certain threshold are available for this analysis. While the threshold for the values $g\Gamma_{\rm n}$, belonging to *s*-wave neutrons, is generally low, in the case of *p*-wave resonances it is, as a rule, substantial and depends on the spin J and the energy $E_{\rm n}$ of a given resonance. It can be shown that the introduction of any *sharp* J- and $E_{\rm n}$-dependent threshold leads to modification of the right-hand sides of Eqs. (5)–(7) and (8b), but after all necessary substitutions into the right-hand side of Eq. (3), the explicit expression for $P(1|g\Gamma_{\rm n})$ remains unchanged. The values of $P(1|g\Gamma_{\rm n})$ are thus completely insensitive to occurrence of this specified threshold.

Using Eqs. (3)–(9) we calculated *a posteriori* probabilities $P(1|g\Gamma_{\rm n})$ for 53 and 72 resonances of ^{107}Ag and ^{109}Ag, respectively. In these calculations we assumed the spin dependence of the level density that follows from the Fermi gas model

$$f(J)=\exp\left(-\frac{J^2}{2\sigma^2}\right)-\exp\left(-\frac{(J+1)^2}{2\sigma^2}\right), \qquad (11)$$

with the spin cutoff factor $\sigma=0.98A^{0.29}$, see Ref. [32]. The values of parameters S_ℓ and $D_{\ell=0}$ were taken from Ref. [5]:

$$S_0=(0.50\pm0.15)\times10^{-4}, \quad S_1=(3.5\pm0.8)\times10^{-4},$$

$$D_{\ell=0}=25\pm3 \ \ \text{eV}$$

for ^{107}Ag, and

$$S_0=(0.84\pm0.23)\times10^{-4}, \quad S_1=(2.8\pm0.8)\times10^{-4},$$

$$D_{\ell=0}=21\pm2 \ \ \text{eV}$$

for ^{109}Ag, where $D_{\ell=0}$ is the average spacing of all *s*-wave resonances.

The values of $P(1|g\Gamma_{\rm n})$ obtained are listed in column 3 of Tables I and II. It is evident, that for 24 and 46 resonances of ^{107}Ag and ^{109}Ag, respectively, these values lead to *s*-wave assignments at a level of statistical significance higher than 99.99%. In all cases of the statistically significant *s*-wave assignments, the results are in full accord with what follows from analyses of the high- and low-energy parts of the γ-ray spectra.

TABLE II. Spin and parity assignment of ^{109}Ag resonances following different methods. The Bayesian probabilities (BP) are given. Under the columns with suffixes HE and LE the ℓ and J assignments from high-energy and low-energy γ-ray methods are indicated, respectively. Under the column J^a are the spin values from Ref. [34]. The adopted values are those with the suffix LE. Resonance energies and neutron widths are taken from Refs. [5,33,34].

E_0 (eV)	$g\Gamma_n$ (meV)	BP	ℓ_{HE}	ℓ_{LE}	J^a	J_{HE}	J_{LE}	E_0 (eV)	$g\Gamma_n$ (meV)	BP	ℓ_{HE}	ℓ_{LE}	J^a	J_{HE}	J_{LE}
30.4	5.4 ± 0.5	0.0000	0	0	1	1	1	446.5				1			2
32.7	0.013 ± 0.002	0.9329	(1)	1			1	469.7	34.5 ± 2.1	0.0000	0	0	0		0
40.1	4.4 ± 0.4	0.0000	0	0	1	1	1	487.0	17.1 ± 1.5	0.0000	0	0		1	1
55.7	5.4 ± 0.5	0.0000	0	0	0		0	500.6	115 ± 11	0.0000	0	0	1		1
70.8	18.9 ± 1.8	0.0000	0	0	1	1	1	512.6	8.6 ± 1.8	0.0000	0	0	0		0
82.5	0.016 ± 0.002	0.9783	1	1			2	526.7	0.70 ± 0.45	0.8414	1	1			1
87.7	4.10 ± 0.3	0.0000	0	0	1	1	1	557.2	13 ± 2	0.0000	0	0		1	1
91.5	0.029 ± 0.003	0.9674		1			2	560.7	66.0 ± 5.5	0.0000	0	0	0		0
106.3	0.14 ± 0.015	0.4658	0	0			0	565.5	69 ± 4	0.0000	0	0	1		1
113.5	0.017 ± 0.004	0.9792		1			2	608.1	25.0 ± 2.5	0.0000	0	0	1		1
133.9	69.1 ± 6.0	0.0000	0	0	1	1	1	622.4	50 ± 35	0.0000	0	0	0	1	1
139.7	1.5 ± 0.5	0.0000	0	0	0	1	1	669.5	18.5 ± 2.0	0.0000		0			1
160.3	0.04 ± 0.01	0.9714		1			1	681.5	2.1 ± 0.5	0.3358		1			2
164.3	0.014 ± 0.005	0.9785		1			2	690.5				1			0
169.8	0.36 ± 0.06	0.1531		1			0	726.1	15.0 ± 1.5	0.0000	0	0		1	1
173.1	33.7 ± 3.0	0.0000	0	0	1	1	1	747.6	54 ± 8	0.0000	0	0			1
199.0	0.11 ± 0.02	0.9428		1			1	784.7	140 ± 15	0.0000	0	0		1	1
209.6	18.6 ± 2.0	0.0000	0	0	1	(1)	1	803.8	25.5 ± 5.5	0.0000	0	0		1	1
219.2	0.06 ± 0.008	0.9678		1			2	821.5				1			2
251.3	4.4 ± 0.4	0.0000	0	0	1	1	1	831.4	3 ± 1	0.2598		1			2
259.0	3.4 ± 0.3	0.0000	0	0			0	848.5			(0)	0			1
264.7	0.18 ± 0.04	0.9290	1	1			2	861.8	8 ± 1	0.0002		0			1
272.6	1.5 ± 0.2	0.0002	0	0		1	1	883.0	55.0 ± 5.5	0.0000	0	0			1
284.0	0.28 ± 0.03	0.8758		1			2	902.8	9 ± 2	0.0001	(0)	0			1
291.0	8.3 ± 0.8	0.0000	0	0	0	1	1	933.0	55 ± 6	0.0000	0	0		1	1
293.3	0.30 ± 0.04	0.8692	1	1			1	949.3	6.0 ± 1.5	0.0151	0	0		1	1
300.9	1.5 ± 0.2	0.0011	0	0			0	961.0	15.5 ± 3.0	0.0000	0	0			0
316.5	150 ± 15	0.0000	0	0	1	1	1	976.0	51.5 ± 4.5	0.0000	0	0		1	1
327.8	0.65 ± 0.07	0.4993	0	0		1	1	1009	66.5 ± 6.5	0.0000	0	0			0
340.2	0.33 ± 0.03	0.8883		1			2	1037	13.5 ± 2.5	0.0000	0	0			1
351.4	0.055 ± 0.006	0.9680		1			2	1057	30.0 ± 3.5	0.0000		0			1
360.4			(0)	0			1	1062	30.0 ± 3.5	0.0000	0	0			0
374.5				1			2	1116	40.0 ± 3.5	0.0000	0	0			1
387.0	41.5 ± 2.0	0.0000	0	0	1		1	1204	130 ± 18	0.0000	0	0		1	1
391.6	0.16 ± 0.02	0.9549		1			1	1219	140 ± 18	0.0000		0			1
398.0	10.0 ± 1.5	0.0000	0	0	1		1	1236	70.0 ± 3.5	0.0000	0	0			1
404.4	42.0 ± 5.0	0.0000	0	0	0		0	1254	17.5 ± 3.5	0.0000	(0)	0			1
428.6	13.7 ± 2.0	0.0000	0	0		1	1	1300	62.5 ± 3.5	0.0000	(0)	0			1
441.0	0.10 ± 0.04	0.9626		1			1	1383	45 ± 5	0.0000	0	0			0

On the other hand, the statistical analysis of quantities $g\Gamma_n$ turned out not to be powerful enough for reliable identification of *p*-wave resonances. However, only in very few cases it might seem that values of $P(1|g\Gamma_n)$ are at variance with parity assignments made by the spectroscopic methods.

It can be concluded that the results of the resonance parity assignment based on the application of the γ- and neutron-spectroscopy methods are compatible. It is evident that the γ-spectroscopy method is substantially more powerful in assignment of the parity value to resonances with lower values of $g\Gamma_n$.

C. Spin assignments

The spin dependence of intensities of low-energy transitions is a well known property of the statistical decay of the compound nucleus, which can be easily observed when low-energy transitions of high enough intensity from levels of

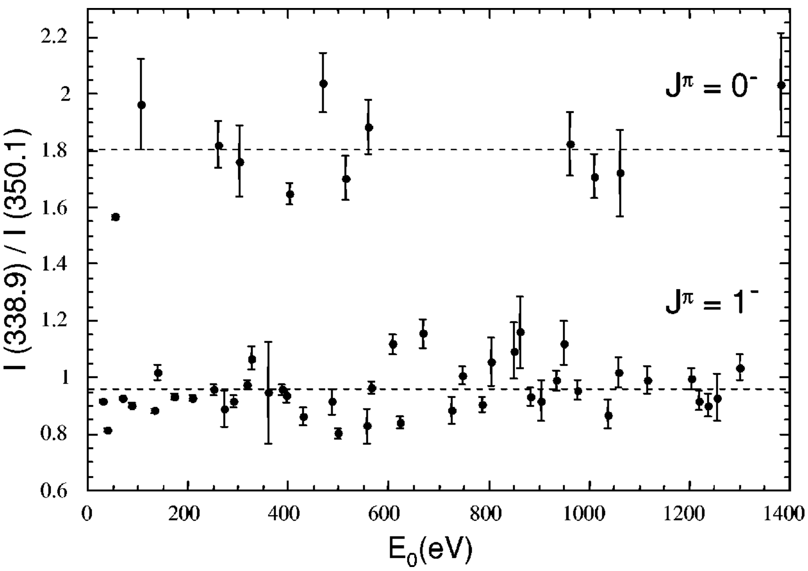

FIG. 7. Ratios of the intensities between γ-ray transitions of 338.9 and 350.1 keV for ^{109}Ag *s*-wave resonances as a function of the resonance energies. The dashed lines are the averages of the groups in which the resonances are split.

different spins are present. As already mentioned, populations of low-energy levels with a given spin are favored when the difference with the resonance spin is low.

For instance, in the case of ^{107}Ag resonances, the transitions of 215.4, 259.3, and 329.2 keV, deexciting levels with spins ranging from 3 to 5, are progressively stronger in resonances with spin 0, 1, and 2, while the opposite happens for the transitions of 193.1 and 300.1 keV, deexciting levels with $J=1$. In the case of ^{109}Ag resonances, strong effects can be observed for the lines of 191.5, the doublet at 235.7 +237.1, 338.9, and 350.1 keV (see Fig. 3).

In order to maximize the spin effect and to avoid any normalization problem, it is customary to calculate the intensity ratio of two transitions from levels with high spin difference. It is also better to consider lines close in energy, in order to avoid possible spurious effects due to change in the shape of the background of the γ spectrum, which could affect the relative intensity of distant lines. In Fig. 7 the intensity ratios between the transitions of 338.9 and 350.1 keV, are plotted as a function of the energy of ^{109}Ag *s*-wave resonances. The ratios split in two groups. The higher values are associated with $J^\pi=0^-$ since the corresponding resonances will tend to populate more the 338.9 keV state, which probably has spin zero, than the state at 468.8 keV with $J^\pi=(2,3)^+$ from which the 350.1 keV transition is emitted. This choice is confirmed by the analysis of high-energy γ rays: many *s* resonances belonging to the lower group in Fig. 7 exhibit strong primary transitions to the level at 198.7 keV, with $J^\pi=2^+$. In fact, with 0^- assignment these primary transitions should be of $M2$ character, which is not realistic. The spin assignment of *s*-wave resonances can also be obtained by considering the ratio of the intensity of the doublet at 235.7+237.1 keV and that of the peak at 191.5 keV, as shown in Fig. 8. There is a one-to-one agreement between the assignments performed using the two different ratios. Because of the higher intensities of the transitions involved, the latter ratio could be used also for the *p* resonances (Fig. 9). In this case the resonances split in three groups, as expected.

The results of the spin assignments of ^{107}Ag and ^{109}Ag resonances are summarized in Tables I and II and compared

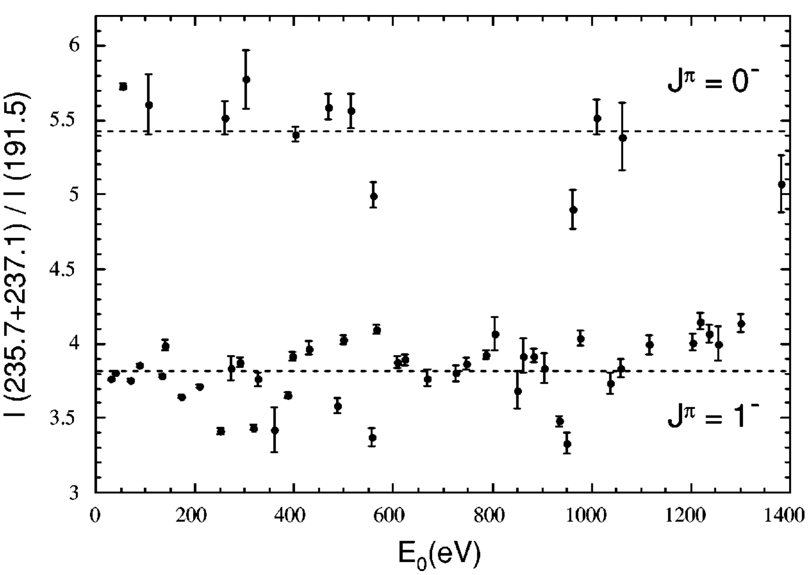

FIG. 8. Ratios of intensities between γ-ray transitions of 235.7 + 237.1 keV and 191.5 keV for ^{109}Ag *s*-wave resonances as a function of the resonance energies.

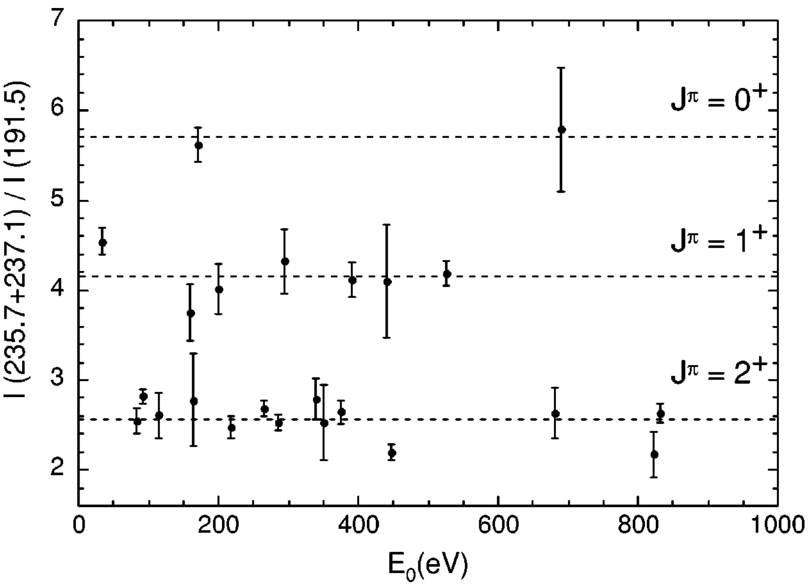

FIG. 9. Intensity ratios between the γ-ray transitions of 235.7 + 237.1 keV and 191.5 keV for ^{109}Ag *p*-wave resonances as a function of the resonance energies. The dashed lines are average values for the various groups of resonances.

with previous data [34] available for some *s* resonances. As can be seen, there are a few disagreements with previous spin assignments of *s* resonances; in these cases our assignment is supported by both low- and high-energy γ rays.

III. COMPARISON WITH RESULTS FROM PARITY VIOLATION EXPERIMENTS

Parity violation effects in Ag resonances have been measured at the LANSCE facility of the Los Alamos National Laboratory [5]. The measured quantity is the *longitudinal asymmetry* $P(E)$:

$$P(E)=\frac{\sigma_T^+-\sigma_T^-}{\sigma_T^++\sigma_T^-}, \tag{12}$$

where $\sigma_T^+(\sigma_T^-)$ is the total cross section, measured using the transmission method, with the neutron spin parallel (antiparallel) to the incident neutron direction. The asymmetry is measured in correspondence to *p*-wave resonances; PV effects are possible in *p* resonances close to *s* resonances of the same spin.

In Ref. [5] a complete discussion on the use on the resonance spins for the analysis of the PV effects is reported. As shown, the knowledge of the resonance spins is very important in reducing uncertainties in the weak spreading width Γ_w, which is the physical quantity of interest. Several *p* resonances showed PV effects with a statistical significance greater than three standard deviations. As an index of the agreement between our results of spin assignment and the observed PV effects, in Fig. 10 the longitudinal asymmetries $P(E)$ divided by their errors $\Delta P(E)$, representing the statistical significance of the PV effects, are plotted for all the *p* resonances to which we assigned the spin. Only the resonances with $J=0,1$ show significant effects, thus indicating an excellent agreement between the two measurements, since *p*-wave resonances with $J=2$ cannot show PV effects.

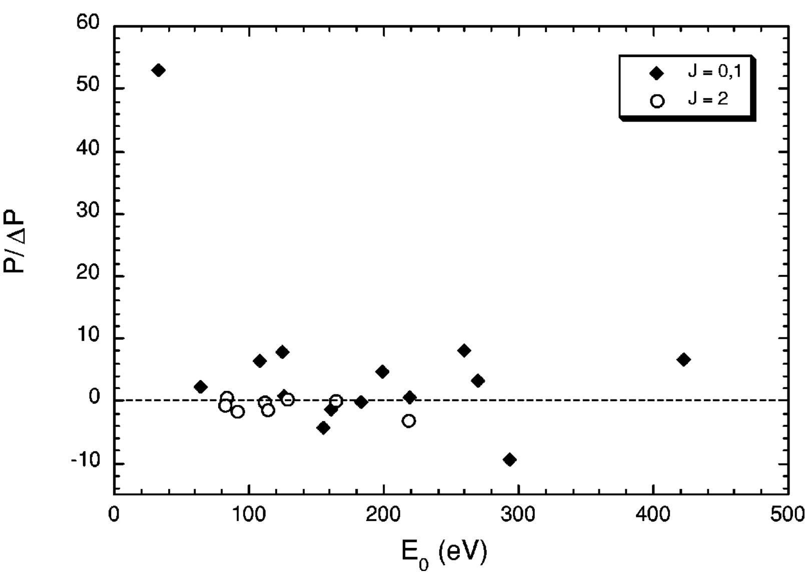

FIG. 10. Statistical significance of PV effects in ^{107}Ag and ^{109}Ag *p* resonances, as a function of the resonance energy. Data from Ref. [5].

IV. CONCLUSIONS

We have studied capture γ rays in ^{107}Ag and ^{109}Ag resonances, with emphasis on low-energy γ rays populated from the cascade γ decay process. We determined the spins and parities of 131 *s*- and *p*-wave resonances of ^{107}Ag and ^{109}Ag.

A clear dependence of the populations of low-energy levels on the parity of the resonance, which was not previously reported, has been observed in both silver isotopes. This effect could be used as a reliable tool for the assignment of the orbital angular momentum of the resonances. This parity effect is also of interest since it can give new information on the $E1$ and $M1$ photon strength functions, as described in another paper [27].

We have shown that the Bayesian approach for the ℓ assignment works reasonably well in the energy range considered; although it is not as reliable as the spectroscopic methods, only a few discrepancies are found with the results from low- and high-energy γ rays.

ACKNOWLEDGMENTS

This paper is based on work carried out at the IRMM in Geel, Belgium. One of the authors (L.Z.) would like to thank Frank Gunsing for helpful discussions.

[1] J. D. Bowman, G. T. Garvey, Mikkel B. Johnson, and G. E. Mitchell, Annu. Rev. Nucl. Part. Sci. **63**, 829 (1993).

[2] G. E. Mitchell, J. D. Bowman, and H. A. Weidenmüller, Rev. Mod. Phys. **71**, 445 (1999).

[3] B. E. Crawford *et al.*, Phys. Rev. C **58**, 1225 (1998).

[4] S. L. Stephenson *et al.*, Phys. Rev. C **58**, 1236 (1998).

[5] L. Y. Lowie *et al.*, Phys. Rev. C **59**, 1119 (1999).

[6] B. E. Crawford *et al.*, Phys. Rev. C **60**, 055503 (1999).

[7] B. J. Allen and A. R. de L. Musgrove, in *Advances in Nuclear Physics*, edited by M. Baranger and E. Vogt (Plenum, New York, 1979), Vol. 10, p. 129.

[8] S. F. Mughabghab, *Proceedings of the Third International School on Neutron Physics* (Alushta, USSR, 1978).

[9] F. Corvi and M. Stefanon, Nucl. Phys. **A233**, 185 (1974).

[10] F. Corvi, M. Stefanon, C. Coceva, and P. Giacobbe, Nucl. Phys. **A203**, 145 (1973).

[11] F. Gunsing, K. Athanassopulos, F. Corvi, H. Postma, Yu. P. Popov, and E. I. Sharapov, Phys. Rev. C **56**, 1266 (1997).

[12] J. M. Salomé, Phys. Mag. **8**, 261 (1986).

[13] J. M. Salomé and R. Cools, Nucl. Instrum. Methods **179**, 13 (1981).

[14] Data acquisition system manual, CMTE-FAST Daten Systeme, GmbH, Munich, Germany, 1990.

[15] F. H. Fröhner, Report KFK-2145, 1976. IRMM revised version by A. Brusegan (private communication).

[16] *PROFIT, Data Analysis and Graphical Presentation on the Macintosh* (Cherwell Scientific Publishing, Oxford, 1996).

[17] D. C. Radford, GF2 fitting program (private communication).

[18] I. A. Kondurov *et al.*, in *Capture Gamma-Ray Spectroscopy*, edited by R. W. Hoff (AIP, Woodbury, NY, 1991), p. 421.

[19] D. De Frenne and E. Jacobs, Nucl. Data Sheets **67**, 809 (1992).

[20] W. T. Eadie, D. Drijard, F. E. James, M. Roos, and B. Sadoulet, *Statistical Methods in Experimental Physics* (North-Holland, Amsterdam, 1971).

[21] L. M. Bollinger and G. E. Thomas, Phys. Rev. **171**, 1293 (1968).

[22] C. M. Frankle, E. I. Sharapov, Yu. P. Popov, J. A. Harvey, N. W. Hill, and L. W. Weston, Phys. Rev. C **50**, 2774 (1994).

[23] F. Gunsing *et al.* (unpublished).

[24] M. Gyulassy, R. J. Howerton, and S. T. Perkins, Report UCRL-50400, Vol. 11 (1972).

[25] H. Postma, Phys. Rev. C **24**, 2322 (1981).

[26] J Honzátko, K. Konečný, I. Tomandl, J. Vacík, F. Bečvář, and P. Cejnar, Nucl. Instrum. Methods Phys. Res. A **376**, 434 (1996).

[27] L. Zanini *et al.* (unpublished).

[28] L. Zanini, Ph.D. thesis, Delft University of Technology, 1998.

[29] A. M. Lane and R. G. Thomas, Rev. Mod. Phys. **30**, 257 (1958).

[30] H. Feshbach, C. E. Porter, and V. Weisskopf, Phys. Rev. **90**, 166 (1953); **96**, 448 (1954).

[31] J. E. Lynn, *The Theory of Neutron Resonance Reactions* (Oxford University, Oxford, 1968).

[32] T. Von Egidy, H. H. Schmidt, and A. N. Behkami, Nucl. Phys. **A481**, 189 (1988).

[33] L. Y. Lowie *et al.*, Phys. Rev. C **56**, 90 (1997).

[34] S. F. Mughabghab, M. Divadeenam, and N. E. Holden, *Neutron Cross Sections* (Academic, New York, 1981).